WOOD RESEARCH doi.org/10.37763/wr.1336-4561/69.4.730743
e-ISSN 2729-8906
69(4): 2024 730-743 pp.

DESIGN AND ANALYSES OF HYBRID FACADE PANELS CREATED WITH TRANSPARENT WOOD BIO-COMPOSITES

JÁN KANÓCZ, VIKTOR KARĽA, MICHAL TOMKO, TOMÁŠ BAROŠ,
VIKTÓRIA BAJZECEROVÁ
TECHNICAL UNIVERSITY OF KOŠICE
SLOVAK REPUBLIC

(RECEIVED NOVEMBER 2024)

ABSTRACT

The paper presents the initial results of research focused on the possibilities of using transparent wood for building envelope structural elements in architecture. Sometheoretical analyses of the hybrid envelope panelsmade with different types of transparent wood were carried out. The aimof the study was to assess static and hygrothermal behaviour of such panels. The panels were considered to be two layers of transparent wood bio-composites each 10 mm thickglued to an oak timber frame with only plain air as insulator in the panel.Because only small samples of transparent wood were produced so far, it was considered that mechanical properties of small samples would be retained in large ones as well.

KEYWORDS:Transparent timber, hybrid structure, hybrid bearing beam, mechanical properties of transparent timber.

INTRODUCTION

Based on previous research on the physical and mechanical properties of transparent wood (TW)(Fink1992, Zhu et al. 2016, Li et al. 2016, Fu et al. 2018, Mi et al. 2019, Le Van et al. 2021, Wang et al. 2018), it is possible to assume their use in the field of building envelope constructions (Katunský et al. 2018). Transparent facade elements are mostly created by using glass, which is less advantageous compared to TW in several ways.If we compare the thermal conductivity and weight of TW with glass, it is evident that in the case of facade elements, for which the mentioned properties are authoritative, the use of TW is more advantageous(Kanócz et al. 2020, Karľa et al. 2022). Especially if reduction of light transmittance, increase of haze and colouration due to UV radiationare not some decisive criterions or are even welcomed(Vasileva et al. 2018, Chen et al. 2019, Wachter et al.

2021,Bisht et al. 2021,Jele et al. 2023). Recent LCA analysis of TW also showed that it has a potential to be favorable from an ecological perspective (Rai et al. 2022) and optimisation of delignification process can contribute to even better sustainability (Qin et al. 2018, Wang et al. 2019, Kohli et al. 2020) as construction sector consumes around 30% of global energy usage (United Nations Environment Programme 2017).

In the initial phase of the research, we focused on the analysis of the dimensional options of the hybrid TW construction panel as a constituent element of the building's façade system. To achieve the optimal dimensions of the TW panel, i.e. length, width and thickness, it was necessary to examine it both from a hygrothermal and physical point of view, as well as from a static point of view. As part of the analyses, several types of TW were used, the mechanical and physical parameters of which are known from the publications of several research teams(Li et al. 2016, Fu et al. 2018, Mi et al. 2019, Le Van et al. 2021, Wang et al. 2018).Five types of TW were considered.Since no TW of larger structural dimensions has been produced so far, the parameters used were determined on small TW samples. The results presented in the article were obtained under the assumption of preserving the mechanical and physical properties of small TW samples even in the case of TW-based structural elements.

Design of the façade panels was influenced by hygrothermal and structural demands. The basic idea was to produce a transparent façade panel, which would only be insulated by an air layer instead of inert gases commonly used in insulation glass windows and curtain walls. This would have multiple advantages, namely improved cost and ecology, as well as simplified production and stable insulation properties throughout the entire life cycle of the façade, as inert gases leak after the years of usage leading to weaker insulation properties of such façade systems over time (Zozuláková et al. 2019, Cho et al. 2023). The aim of the article is to assess whether such façade panels would be a feasible option for the future applications.

MATERIALS AND METHODS

Design of façade elements

The dimensions of the investigated façade panels for the case of a standard skeletal support system with a structural height of 3 mwere designed. For such a construction, two suitable size series of panels were chosen. Panels for the full structural height have dimensions of 1200 x 3000 mm, and panels with half the structural height with dimensions of 600 x 1500 mm weredesigned.For determining the cross-section dimensions of the panel´s wooden frame, the starting point was the minimalwidth of the air gap between the TW panesmeetingthe hygrothermal requirements and sufficient static resistance.Foran initialthermal transmittance analysis, the designed frame of the panel was glued oak timber with a cross section of 40 x 40 mm with groove and tongue. As a next stepof hygrothermal analysis,the frame with a 40 x 60 mm cross sectionwas considered. The thickness of TW panes was set at 10 mm for both sidesof each panel (Fig. 1).

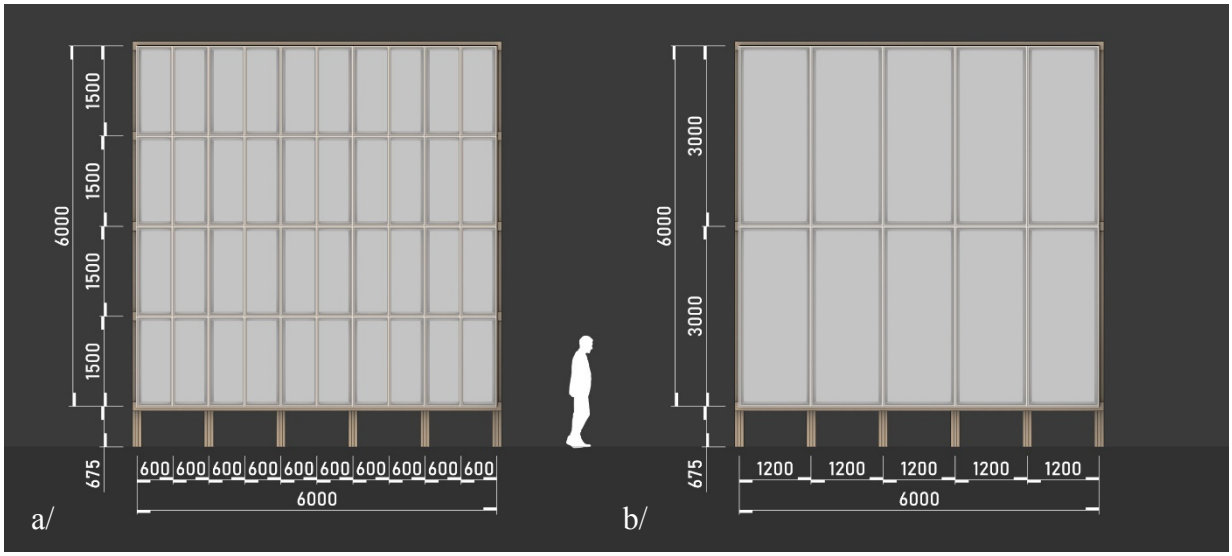

Fig. 1: Dimensions of TW façade:a) panels 600 x 1500 mm, b) panels 1200 x 3000 mm.

Characteristicsoftransparent wood veneers

For the analysisof façade panel various types of transparent woodwere considered.The properties of small transparent woodsamples were taken from articles describing respective transparent wood types. The types were sorted into four categories based on the polymer impregnated into the delignified wood: *(1)*balsa wood impregnated with PMMA (poly methylmetacrylate) (Li et al. 2016), *(2)*balsa wood impregnated with PVA (polyvinyl alcohol) (Mi et al. 2019), *(3)*fir wood impregnated with CTS (chitosan) (Le Van et al. 2021),*(4)*fir wood impregnated with CNF (cellulose nano fibres) (Le Van et al. 2021).For each category, transparent plywood with 90° orientation of layers was chosen as an assessed material in façade elements.

Additionally, transparent fibrewood (TFW) (Wang et al. 2018) was also considered, as it is regarded to be the most feasible option because preparation of large samples is less difficult in this case, although it is structurally less favourable.However, not all properties required for the analyses were available from the above mentioned articles.Considering structural analysis, tensile strength and Young's modulus were available, but shear modulus, Poisson's ratio and mass were not. Volumes of cellulose and polymer in the final samples of TW were considered to be 12% and 88%, resp. Mass and Poisson's ratio in longitudinal direction were then calculated as the weighted average of respective wood kinds and polymers.Poisson's ratio μ(-) in transverse direction was calculated according to equation:

$$\mu_{transverse} = \mu_{longitudinal} \times E_{transverse} \div E_{longitudinal} \qquad (1)$$

where:$\mu_{longitudinal}$ is Poisson's ratio in longitudinal direction [-], $E_{transverse}$ is Young's modulus in transverse direction [GPa], $E_{longitudinal}$ is Young's modulus in longitudinal direction [GPa].

Shear moduli G [GPa] for each direction were then calculated according to equations:

$$G_{longitudinal} = \frac{E_{longitudinal}}{2(1+\mu_{longitudinal})} \quad (2)$$

$$G_{transverse} = \frac{E_{transverse}}{2(1+\mu_{transverse})} \quad (3)$$

where: $\mu_{transverse}$is Poisson's ratio in transverse direction [-], $\mu_{longitudinal}$ is Poisson's ratio in longitudinal direction [-], $E_{transverse}$ is Young's modulus in transverse direction [GPa], $E_{longitudinal}$ is Young's modulus in longitudinal direction [GPa]. Properties of considered TW veneers are listed in Tab. 1.

Tab. 1: Mechanical properties of considered TW veneers.

Material	Original wood	Fibers' direction	Young's modulus *E (GPa)*	Shear modulus *G (GPa)*	Poisson's ratio *μ (-)*	Tensile strength *F (MPa)*	Mass m (kgm^{-3})	Thermal conductivity coefficient *λ* ($Wm^{-1}K^{-1}$)
TW PMMA	Balsa	Longit.	4.3	1.57	0.37	62.5	1060	0.23
		Transv.	2.4	0.99	0.21	14.6		
TW PVA	Balsa	Longit.	3.85	1.33	0.45	143	1070	0.39
		Transv.	3.1	1.14	0.36	67		
TW CTS	Fir	Longit.	10.81	4.09	0.32	171.85	1590	-
		Transv.	3.48	1.58	0.1	26.5		
TW CNF	Fir	Longit.	15.33	5.51	0.39	258.84	1330	-
		Transv.	4.07	1.85	0.1	31.27		
TFW PMMA	Poplar	-	2.2	0.9	0.23	46.8	1080	0.178

Characteristics of transparent plywood

Considering transparent plywood materials (TPW), there were some data on PMMA infiltrated transparent plywood (Fu et al. 2018), namely tensile strength and Young's modulus. Poisson's ratio and shear modulus were then calculated with ABD matricesusing an online matrix calculator at *www.app.abdcomposites.com*.Other types of transparent wood lacked any data on their transparent plywood counterparts. Their tensile strengths were therefore calculated according to laminate theory (Nettles1994) usingequations:

$$F_{TPW\ longitudinal} = \frac{3F_{TW\ longitudinal}}{5} + 0{,}1\frac{2F_{TW\ transverse}}{5} \quad (4)$$

$$F_{TPW\ transverse} = \frac{2F_{TW\ longitudinal}}{5} + 0{,}1\frac{3F_{TW\ transverse}}{5} \quad (5)$$

where: $F_{TPWlongitudinal}$is tensile strength of transparent plywood in longitudinal direction [MPa], $F_{TPWtransverse}$ is tensile strength of transparent plywood in transverse direction [MPa], $F_{TWlongitudinal}$is tensile strength of TW veneer in longitudinal direction [MPa], $F_{TWtransverse}$ is tensile strength of TW veneer in transverse direction [MPa].

Then, Young's moduli E [GPa], Poisson's ratios μ [-] and shear moduli G [GPa] were calculated using the above-mentioned matrix calculator. Mass was considered to be the same as it was for the corresponding single layer transparent wood veneers.

For the thermal analyses, there were some data available on thermal conductivity coefficients for PMMA and PVA infiltrated transparent wood bio-composites. Other TW bio-composite types lack these data. Another required datawere missing completely. However, water vapor diffusion resistancefactor was consideredas 94 000 and specific heat capacity was considered as 1465 $Jkg^{-1}K^{-1}$, which arecommon values for plastic materials.Properties of TPW materials are listed in Tab. 2.

Tab. 2: Mechanical properties of TPW (each plywood material is considered 10 mm thick, with 5 layers, each layer 2 mm thick having 90° orientation of layers) and TFW materials used in analyses.

Material	Original wood	Fibers' direction	Young's modulus *E (GPa)*	Shear modulus *G (GPa)*	Poisson's ratio *μ (-)*	Tensile strength *F (MPa)*	Mass m (kgm^{-3})	Thermal conductivity coefficient *λ* ($Wm^{-1}K^{-1}$)
TPW PMMA	Balsa	Longit.	4.1	1.6	0.28	50.1	1060	0.23
		Transv.	3.9	1.54	0.27	44.9		
TPW PVA	Balsa	Longit.	3.56	1.33	0.41	88.48	1070	0.39
		Transv.	3.41	1.23	0.39	61.22		
TPW CTS	Fir	Longit.	7.95	4.09	0.17	104.17	1590	-
		Transv.	6.47	2.84	0.14	70.33		
TPW CNF	Fir	Longit.	10.93	5.51	0.16	156.55	1330	-
		Transv.	8.66	3.83	0.13	105.41		
TFW PMMA	Poplar	-	2.2	0.9	0.23	46.8	1080	0.178

Structural analysis

Panels created with transparent plywood of all types and transparent fibrewood listed in Tab. 2 were subject of the analysis. We proceeded to the calculation of a 600x1500x60 mm panel with an air gap of 40 mm. To calculate the panel, we used the TW with the highest and the lowest value of the modulus of elasticity, i.e. TWP CNF and TFW PMMA. Based on the obtained calculation results in the case of 1200x3000x80 mm panels, to limit excessive deflection of TWpane, the wooden frame with a horizontal bar in the middle of the frame as well as a diagonal bar across the entire height of the panel were supplemented (Fig. 2). In the case of each type of frame – without inner bar (A), with horizontal bar (B) and with diagonal bar (C), all types of TW from Tab. 2 were used.

Within the numerical model, the wind load effect, the point discrete force effect and the thermal expansion effect were considered.The wind load was calculated based on the Eurocode 1, STN EN 1991-1-4 standard. The final wind load was defined with value of 1.5 kPa.

In the case of beams with length L= 1500mm and L= 3000mm without reinforcements with TW panes of types TPW CNF and TFW PMMA, in addition to wind load, we looked at the response from the effect of a single load and the effect of temperature. We considered a discrete force of magnitude 3.5kN acting perpendicular to the plane of the panel at its centre. The thermal load represented a temperature difference of 20°C.

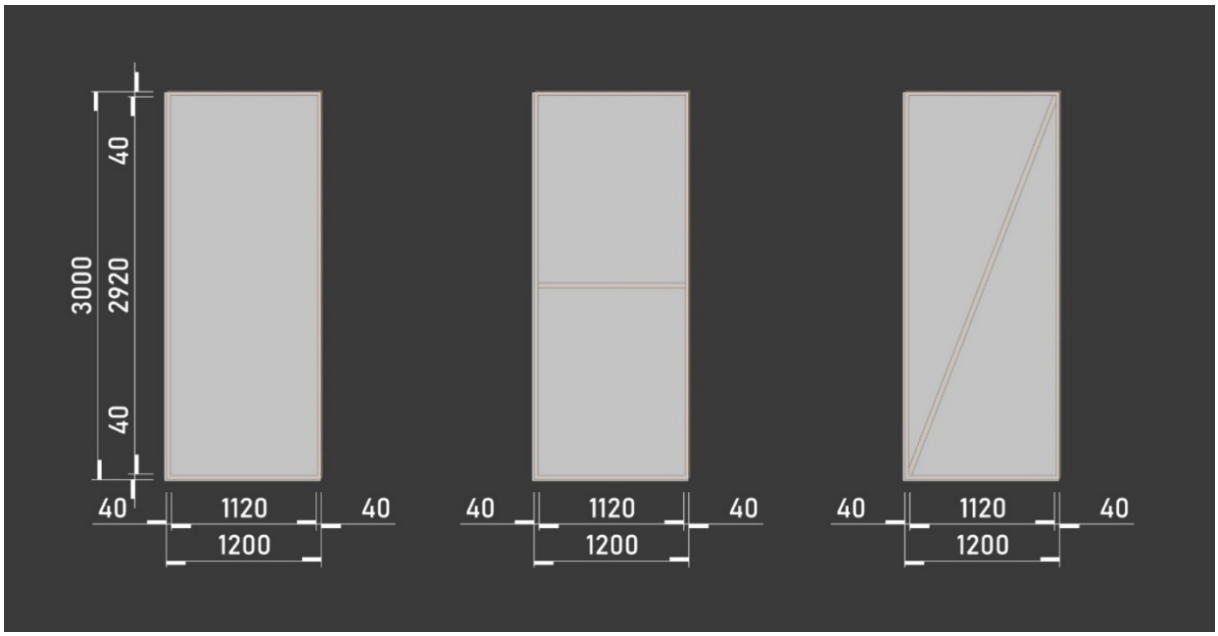

Fig. 2: Dimensions of 1200 x 3000 mm panel: a/ panel type A, b/ panel type B, c/ panel type C.

The static analysis in the Ansys 2024 program was carried out. A spatial model was created from 3D finite elements of the Solid186 type. The maximum size of the final elements was 20 mm. Boundary conditions were imposed on the upper and lower wooden frames by preventing displacements in all directions, x,y,z. The model contained 38469 3D elements and 167575 finite element mesh nodes. The contact elements between the wooden frame and the transparent wood were created through rigid contact (glue) - type bonded.

Analyses of hygrothermal behaviour

According to STN 73 0540-2+Z1+Z2, required thermal transmittance(U-value) for glazing is 0,85 $Wm^{-2}K^{-1}$and recommended is 0.65 $Wm^{-2}K^{-1}$. U-value of transparent wood bio-composite façade panelwas calculated by Eqs. 6 and 7:

$$U = \frac{1}{R} \quad (6)$$

$$R = \sum \frac{d}{\lambda} \quad (7)$$

where:R is thermal resistance [$Wm^{-2}K^{-1}$], d is thickness of a material[m],λ is thermal conductivity coefficient[$Wm^{-2}K^{-1}$].

As the air layer in façade panel also consists ofglued oak timber frame, thermal conductivity coefficient λ [$Wm^{-2}K^{-1}$] was calculated as an average of oak and air coefficient weighted by their corresponding areas.The U-values [$Wm^{-2}K^{-1}$] were calculated for each type of designed panels and thermal conductivity coefficient λfor transparent wood layer was set to 0.39 $Wm^{-2}K^{-1}$, as it is the least favourable of the available coefficients. For air, the coefficient was 0.0262$Wm^{-2}K^{-1}$and for glued oak it was 0.22 $Wm^{-2}K^{-1}$.

Additionally, a HAM (Heat Air Moisture) simulation was run using WUFI 2D software where the proposed structure's behavioural characteristics regarding heat and moisture transport were analysed. The structure in question was defined as a transparent wall structure. The resulting courses describe the temporal evolution of the monitored quantities from profiles showing the quantity distribution across the building component over time. Three parameters were monitored (surface temperature on the interior and exterior panels of the transparent panel, relative humidity in the closed air gap and water content on the inner surfaces of the transparent panels and the air gap and each layer of the structure). The criteria for assessing the structure in question were compliance with the hygiene criterion (i.e. that there will be no condensation on the inner surface of the structure), meeting the condition of a favourable annual balance of possible condensation of water vapour into the structure Mc and evaporated moisture from the structure Mev throughout the year (i.e. the annual amount of condensed water vapour inside the structure Mc in kg/(m^2.a) must be lower than the annual amount of water vapour that can evaporate Mev in kg/(m^2.a). Mc < Mev); limited condensation of water vapour in the structure was also considered, which is determined without considering the influence of solar radiation, provided that condensation occurs in the structure.The condensed water vapour does not endanger the structure's required function, and the permissible annual amount of condensed water vapour is Mc < 0.5 kg/(m^2.a). The assessed structure is considered in a space with a relative air humidity of $\varphi i \leq 50\%$ and must have a surface temperature $\theta si,w$ above the dew point temperature $\theta dp = 9.26°C$ at each location, corresponding to the calculated indoor air temperature θai and the relative indoor air humidity φi. Meeting the requirement for the critical temperature of the risk of mould growth is considered to meet the hygiene criterion. Material parameters were defined from WUFI embedded databases, and boundary conditions were external conditions (climate: meteorological data from Košice airport, orientation: north), internal conditions (sinusoidal curve selection: medium moisture load; average internal temperature: 21°C, amplitude 1K; relative humidity: 50%, amplitude 10%), and adiabatic boundary. The calculation was performed in hourly steps for 10 years.

RESULTS AND DISCUSION

Static analysis results

As part of the static analysis, we focused on investigating the deformation properties as well as the spatial stresses of the designed panels. We investigated the panel´s total deflections (Fig. 3), deflections and normal stresses of TW panes (Fig. 4). The results obtainedby the numerical analysis of the 600x1500x60 panels showed (Tab. 3) that while the

tension of TW is almost identical for both panels, their total deflections are significantly different. The total deflection value of TFW PMMA pane is 389% greater than the total deflection of TPW CNF. Based on this comparison, it can be assumed that all types of TW panes presented above will have a deflection in the range of 0.7 mm to 2.84 mm. The maximum normal stresses in both calculated cases were reached in the direction of the shorter dimension of the panel. In the case of TPW CNF it is the direction perpendicular to the fibres and the maximum tensile stress is in size of 1.57% of the tensile strength of TW PMMA material. In the case of TFW PMMA, the tensile strength is constant in all directions, and the measured values are at the level of 3.88% of the tensile strength. From the above results, it follows that the deflection of the TW panes will be a decisive static point of view for designing TW panels. Total deflections of TW panes in Tab. 3 are smaller than L/500, therefore it can be assumed that, when assessed using limit state criteria, each panel with TW panes from Tab. 2 would fit statically.

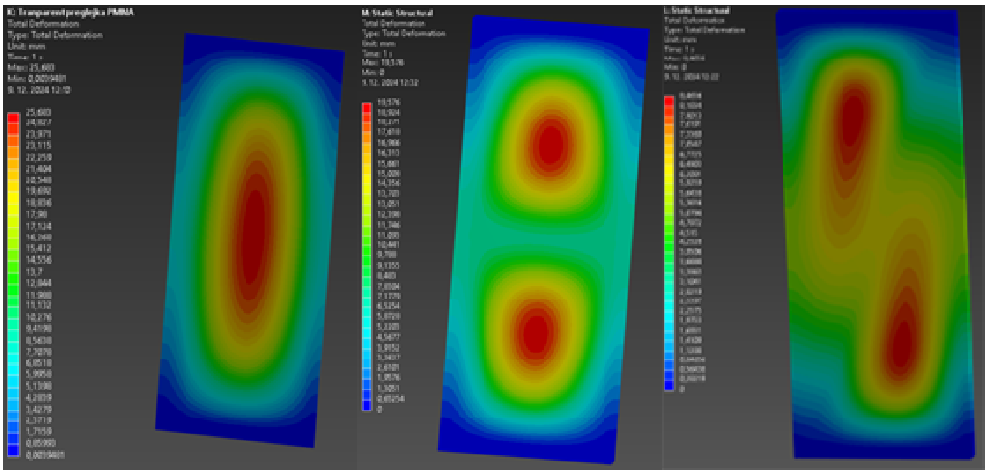

Fig. 3: Total deflection of the panels with TPW PMMA - a/ type A, b/ type B, c/ type C.

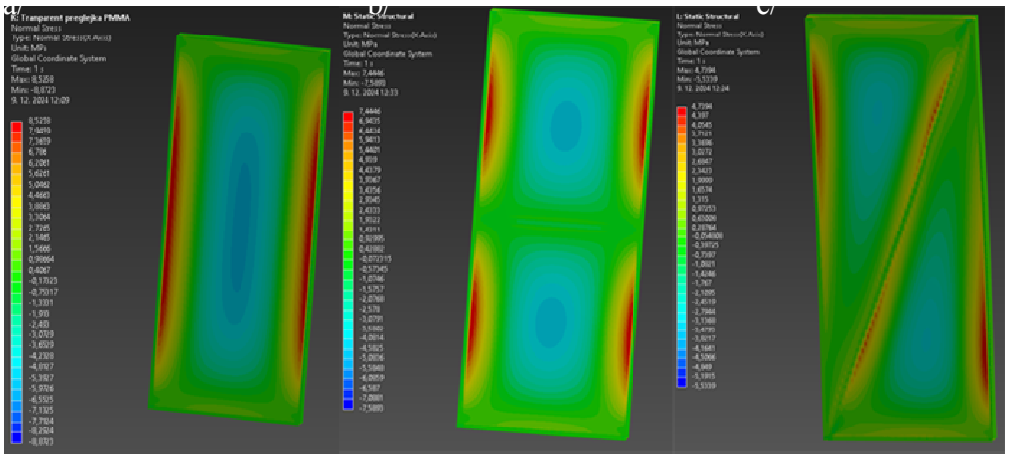

Fig. 4: Normal stress of the panels with TPW PMMA - a/ type A, b/ type B, c/ type C.

Tab. 3:Results of static analysis of 600 x 1500 x 60 mm façade panels.

Pane material	Tot. def. of TW pane[mm]	Max. tensile stress[MPa]	Max. comp. stress[MPa]
TPW CNF	0.73	1.66	-1.76
TFW PMMA	2.84	1.82	-1.76

In the next phase of the analysis, TW panels with dimensions of 1200x3000x80 mm were the subject of investigation. Like in the case of shorter panels, we started numerical calculations with panels – type A, where we used TPW CNF and TFW PMMA panes. Due to the experience with shorter panels, we focused on monitoring the total deflections. The obtained values showed that the total deflection of the TPW CNF pane is 25.68 mm, which corresponds to a deflection of L/300. In the case of the TFW PMMA pane, the total deflection reached 44.33 mm, which is a deflection of L/68. This value is already significant and unsatisfactory from the point of view of the usability of the panel. After inserting the horizontal element in the middle of the wooden frame – type B panel, the total deflection of the TFW PMMA pane was reduced to 30.73 mm, and after inserting the diagonal element into the wooden frame of the panel - type C, there was a further reduction of the total deflection to a value of 13.23 mm. These valuesrepresent 30.8% and 70.2% reduction of the frame deflection without reinforcement resp.

Next panels of types A, B, and C with TPW panes of PMMA, PVA, and CTS were subjected to numerical analysis. The total deflections of all calculated TW panes with L = 3000 mm are shown in the graph in Fig.5, from which it is possible to see how their total deflection decreases by adding reinforcing rods to the wooden perimeter frame. If we set L/300 as the limit deflection of TW panes for their practical use, then it can be concluded that this criterion is met by the panel type A with TPW CFN panes. In the case of a reinforced panel of type B, panels with TPW CTS and TPW CNF panes and in the case of a panel of type C, every panel except for a panel with TFW PMMA meets the mentioned criterion.

The method of distribution of normal stresses in TW panes is different for individual types of panels. In principle, it can be stated that the maximum compressive stresses appear above the wooden frames in the places where the frames have maximum deformation. These stresses are almost identical for individual TW panes in individual types of frames and their values range from 5.21 MPa to 8.93 MPa. The maximum tensile stresses are found in the places of total deflection of TW panes and their values range from 4.18 MPa to 8.52 MPa. The stated values are significantly lower than the tensile strength of individual types of TW in Tab. 2.

Tab. 4: Results of static analysis of 1200 x 3000 x 80 mm façade panels.

Panel type	Pane material	Tot. def. of TW pane [mm]	Tot. def. of frame [mm]	Tot. def. of bracing [mm]	Max. tensile stress [MPa]	Max. comp. stress [MPa]
Panel type A	TPW PMMA	25.68	6.97	-	8.52	-8.87
	TPW PVA	25.77	5.97	-	8.36	-8.92
	TPW CTS	13.93	3.5	-	8.38	-8.93
	TPW CNF	10.38	2.73	-	8.36	-8.92
	TFW PMMA	44.33	8.46	-	8.43	-8.89

Panel type B	TPW PMMA	19.57	7.06	7.72	7.44	-7.58
	TPW PVA	18.15	6.14	6.86	6.56	-6.98
	TPW CTS	10.23	3.61	4.05	6.8	-7.3
	TPW CNF	7.68	2.8	3.15	6.89	-7.34
	TFW PMMA	30.73	8.55	9.79	6.71	-6.88
Panel type C	TPW PMMA	8.46	5.25	6.25	4.73	-5.53
	TPW PVA	7.99	4.3	5.33	4.18	-5.21
	TPW CTS	4.5	2.6	3.12	4.31	-5.29
	TPW CNF	3.41	2.04	2.44	4.34	-5.24
	TFW PMMA	13.23	5.96	7.47	4.38	-5.87

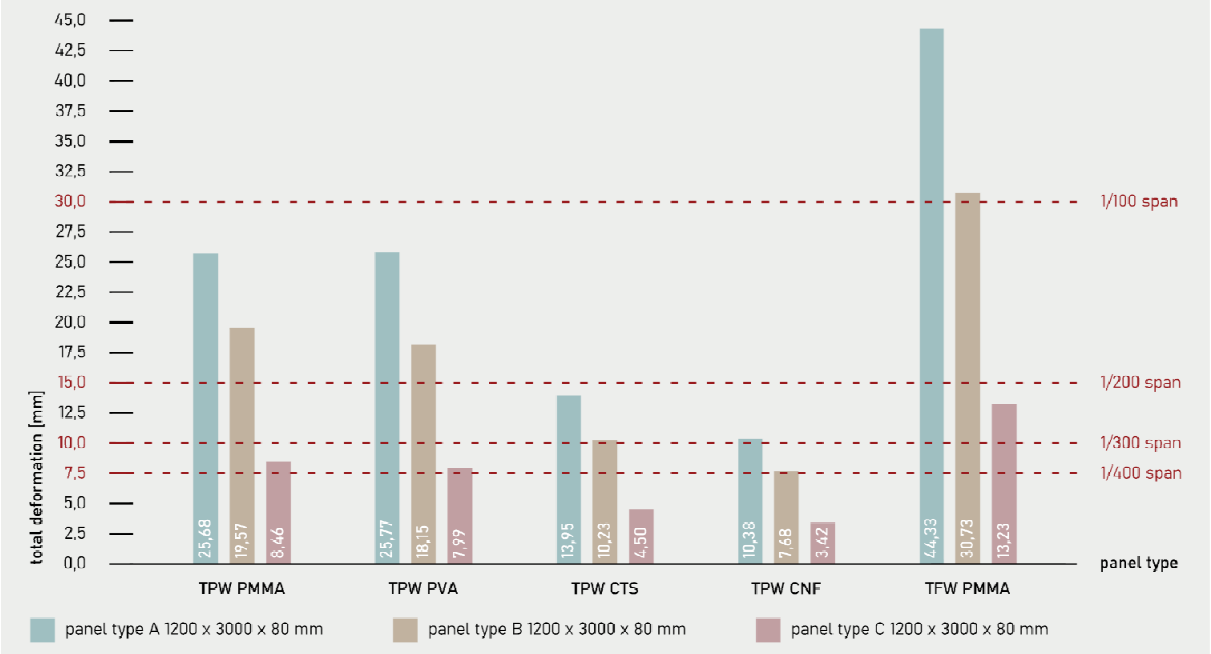

Fig. 5: Total deflections of 1200 x 3000 x 80 mm TW panes.

Hygrothermal analysis results

Thermal transmittances (U-values) of designed transparent wood bio-composite façade panels are listedinthe Tab. 5. The small 600 x 1500 x 60 mm panel meetsthe requirement of the standard while600 x 1500 x 80 mm panel already meets standard recommendation.All the large 1200 x 3000 x 80 mm panels meet the standard recommendation with a U-value as low as 20 – 21% of the standardized recommended valueand15.5 –16% of the standardized required value.

Tab.5: Thermal transmittance values (U-values) of transparent wood bio-composite façade panels (thermal conductivity coefficient λ for TW was considered 0.39 $Wm^{-1}K^{-1}$).

Panel type	**Panel U-value ($Wm^{-2}K^{-1}$)**
Panel 600 x 1500 x 60 mm	0.826*
Panel 600 x 1500 x 80 mm	0.558**
Panel type A 1200 x 3000 x80 mm	0.132**
Panel type B 1200 x 3000 x 80 mm	0.134**
Panel type C 1200 x 3000 x 80 mm	0.137**

*Standard required U-value is 0.85 $Wm^{-2}K^{-1}$.
**Standard recommended U-value is 0.65 $Wm^{-2}K^{-1}$.

According to HAM simulation,assessed structures comply to the standards. Minimal surface temperature θsi,w for the 1200 x 3000 x 80 mm panel was 10.23 °C, which is higher than dew point temperature θdp = 9.26 °C. It is also true for the 600 x 1500 x 60 mm panel, where minimal surface temperature θsi,w was 10.13 °C. The annual amount of condensed water vapour Mc was lower than 0.5 kg/m^2.aover the full span of simulation (10 years). It is obvious over the course of simulation, that the annual amount of condensed water vapourMc is lower than amount of evaporated moisture from the structure Mev, as moisture content levels are declining with time for both panel sizes, as is visible at Fig. 6 and listed in Tab. 6.

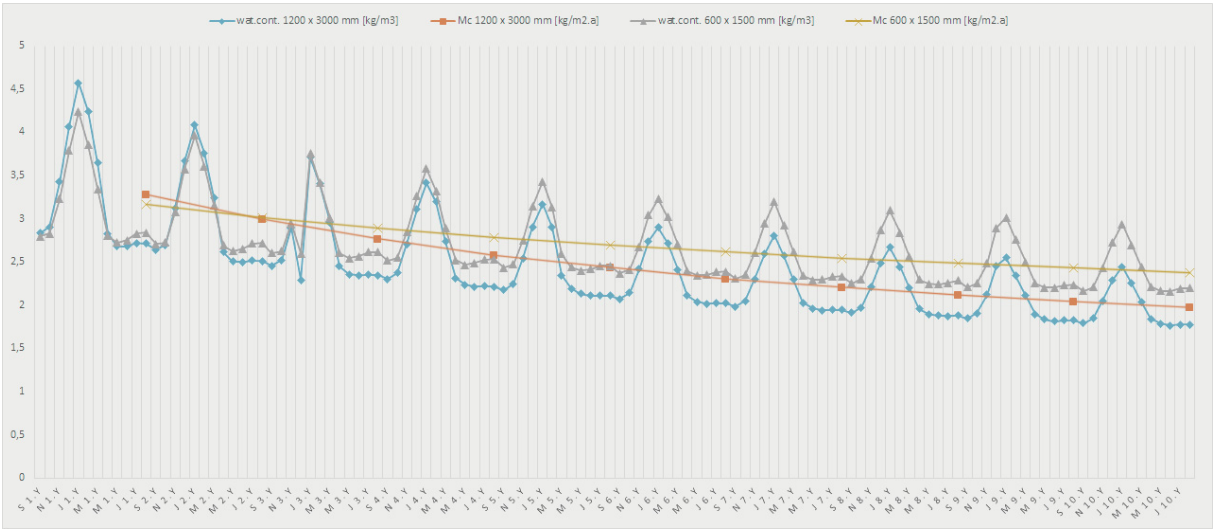

Fig. 6:Moisture content levelsof façade panels over the period of ten years.

Tab. 6: Water content levels of façade panels over the period of ten years.

Panel type	Year	Monthly water content [kg/m^3]												Mc [kg/m^2.a]
		Sep	Oct	Nov	Dec	Jan	Feb	Mar	Apr	May	Jun	Jul	Aug	
600 x 1500 x 60 mm	1	2.79	2.83	3.23	3.79	4.24	3.85	3.34	2.80	2.72	2.75	2.83	2.84	3.17
	2	2.71	2.72	3.08	3.57	3.97	3.61	3.16	2.69	2.63	2.65	2.72	2.72	3.02
	3	2.61	2.63	2.95	2.60	3.75	3.41	3.01	2.60	2.54	2.57	2.61	2.62	2.89
	4	2.52	2.55	2.84	3.26	3.58	3.32	2.89	2.52	2.47	2.49	2.53	2.53	2.78
	5	2.43	2.47	2.75	3.14	3.43	3.13	2.59	2.44	2.40	2.42	2.45	2.46	2.69
	6	2.37	2.41	2.67	3.04	3.23	3.02	2.70	2.40	2.34	2.35	2.39	2.39	2.61
	7	2.31	2.35	2.60	2.95	3.19	2.92	2.62	2.34	2.29	2.30	2.33	2.33	2.54
	8	2.25	2.30	2.54	2.87	3.10	2.84	2.56	2.29	2.25	2.24	2.26	2.28	2.48
	9	2.21	2.25	2.48	2.89	3.01	2.76	2.50	2.25	2.20	2.20	2.23	2.24	2.43
	10	2.16	2.21	2.43	2.73	2.94	2.70	2.44	2.21	2.16	2.16	2.19	2.20	2.38
1200 x 3000 x 80 mm	1	2.83	2.90	3.42	4.07	4.57	4.24	3.64	2.83	2.68	2.68	2.72	2.71	3.27
	2	2.64	2.70	3.13	3.66	4.08	3.76	3.25	2.61	2.50	2.50	2.52	2.51	2.99
	3	2.46	2.52	2.89	2.29	3.71	3.40	2.96	2.45	2.36	2.35	2.35	2.35	2.76
	4	2.30	2.37	2.70	3.11	3.41	3.19	2.73	2.32	2.23	2.22	2.22	2.22	2.58
	5	2.17	2.25	2.54	2.91	3.17	2.90	2.35	2.19	2.13	2.11	2.11	2.11	2.43
	6	2.07	2.14	2.41	2.74	2.90	2.72	2.41	2.11	2.04	2.01	2.02	2.02	2.30
	7	1.98	2.05	2.30	2.60	2.81	2.57	2.29	2.03	1.96	1.94	1.95	1.95	2.20
	8	1.91	1.97	2.21	2.48	2.67	2.45	2.20	1.96	1.90	1.88	1.88	1.88	2.11
	9	1.85	1.91	2.12	2.45	2.55	2.34	2.11	1.89	1.84	1.81	1.82	1.83	2.04
	10	1.79	1.85	2.05	2.29	2.45	2.25	2.04	1.84	1.79	1.76	1.78	1.78	1.97

CONCLUSIONS

The presented theoretical analyses showed that transparent wood is an interesting material having properties readyto be used for building envelopes and is suitable for building industry, provided that large samples will be produced in the future. The static analyses proved that the challenge for transparent wood is its low Young's modulus, resulting in greater deformation of large panes, but as it shows, it can be battled by smart addition of bracing into panels. Although transparent fibrewood is the most promising wayto upscale transparent wood bio-composites, it shows that large panels would be difficult to build unless the expectations for max. deformation would be lowered to at least 1/200 span. For smaller panels, allthe investigated types of transparent plywood and transparent fibrewoodbio-composites show more than satisfactory results in their static behaviour.

Hygrothermal analyses proved that proposed façade panels fulfil the requirements of the standard, with most panel types even being able to fulfil the recommendations of STN 73 0540-2+Z1+Z2. Furthermore, hygrothermal analyses proved that the façade panels would also fulfil hygienic criteria set for transparent structures and that humidity inside panels would decline over the years.

ACKNOWLEDGEMENTS

This work was supported by the Scientific Grant Agency of the Ministry of Education, Science, Research and Sport of the Slovak Republic and the Slovak Academy of Sciences under Projects VEGA 1/0626/22 and KEGA 030TUKE-4/2022.

REFERENCES

1. Fink, S. (1992). Transparent Wood – A New Approach in the Functional Study of Wood Structure.Holzforschung, vol. 46, no. 5, 1992, pp. 403-408.
2. Mingwei Zhu, Jianwei Song, Tian Li, Amy Gong, Yanbin Wang, Jiaqi Dai, Yonggang Yao, Wei Luo, Doug Henderson, Liangbing Hu (2016). Highly anisotropic, highly transparent wood composites. Advanced Materials, 28(26), 5181–5187.
3. Yuanyuan Li, Qiliang Fu, Shun Yu, Min Yan, and Lars Berglund (2016). Optically Transparent Wood from a Nanoporous Cellulosic Template: Combining Functional and Structural Performance. Biomacromolecules, 17, 1358-1364.
4. Fu, Q., Yan, M., Jungstedt, E., Yang, X., Li, Y., & Berglund, L. A. (2018). Transparent plywood as a load-bearing and luminescent biocomposite. Composites Science and Technology, 164, 296-303.
5. Wang, Xuan, Zhan, Tianyi, Liu, Yan, Shi, Jiangtao, Pan, Biao, Zhang, Yaoli, Cai, Liping, Shi, Sheldon (2018). Large□Size Transparent Wood for Energy□Saving Building Applications. ChemSusChem, 5, 3855-3862.

6. Mi, Ruiyu, Li, Tian, Dalgo, Daniel,Chaoji, Chen, Kuang, Yudi, He, Shuaiming, Zhao, Xinpeng, Xie, Weiqi, Gan, Wentao, Zhu, J.Y.,Srebric, Jelena, Yang, Ronggui, Hu, Liangbing. (2019). A Clear, Strong, and Thermally Insulated Transparent Wood for Energy Efficient Windows. Advanced Functional Materials, 30, 1907511.
7. Le Van, Hai, Mwongeli, Ruth, Panicker, Pooja,Agumba, Dickens, Pham, Hoa, Kim, Jaehwan. (2021). All-biobased transparentwood: A new approach and its environmental-friendly packaging application. Carbohydrate Polymers, 264, 118012.
8. Katunský, D., Kanócz, J., Karľa, V. (2018). Structural Elements with Transparent Wood in Architecture. International Review of Applied Sciences and Engineering = IRASE, 2, 101-106.
9. Kanócz, J., Bajzecerová, V., Karľa, V. (2020) Analysis of mechanical properties of I-beam with web from transparent wood. IOP Conf. Seri.Mater. Sci. Eng. 2020, 867, 012017.
10. Viktor Karľa, Viktória Bajzecerová, Ján Kanócz (2022). Potential Use of Transparent Wood in Spatial Folded Structures. IOP Conf. Ser.: Mater. Sci. Eng., 1252 012001
11. Vasileva E, Chen H, Li Y, Sychugov I, Yan M, Berglund L, Popov S (2018) Light scattering by structurally anisotropic media: a benchmark with transparent wood. Adv Opt Mater 6:1800999.
12. Chen H, Baitenov A, Li Y, Vasileva E, Popov S, Sychugov I, Yan M, Berglund L (2019). Thickness dependence of optical transmittance of transparent wood: chemical modification effects. ACS Appl Mater Interfaces 11:35451–35457.
13. Wachter I, Štefko T, Rantuch P, Martinka J, Pastierová A (2021) Effect of UV radiation on optical properties and hardness of transparent wood. Polymers 13:2067.
14. Bisht P, Pandey KK, Barshilia HC (2021). Photostable transparent wood composite functionalized with an UV-absorber. PolymDegrad Stab 189:109600.
15. Jele, T.B., Andrew, J., John, M. et al (2023). Engineered transparent wood composites: a review. Cellulose 30, 5447–5471.
16. Rohit Rai, Rahul Ranjan, Prodyut Dhar (2022), Life cycle assessment of transparent wood production using emerging technologies and strategic scale-up framework. Science of The Total Environment, Volume 846, 157301.
17. Jiankun Qin, Xiaowan Li, Yali Shao, Kaixin Shi, Xin Zhao, Tianshi Feng, Yingcheng Hu (2018). Optimization of delignification process for efficient preparation of transparent wood with high strength and high transmittance. Vacuum, Volume 158, Pages 158-165.
18. Wang M, Li R, Chen G, Zhou S, Feng X, Chen Y, He M, Liu D, Song T, Qi H (2019) Highly stretchable, transparent, and conductive wood fabricated by in situ photopolymerization with polymerizable deep eutectic solvents. ACS Appl Mater Interfaces 11:14313–14321.
19. Kirtika Kohli, Sarmila Katuwal, Atanu Biswas, Brajendra K. Sharma (2020). Effective delignification of lignocellulosic biomass by microwave assisted deep eutectic solvents. Bioresource Technology, Volume 303, 122897.
20. United Nations Environment Programme (2017) Global Status Report 2017 - Towards a Zero-Emission, Efficient, and Resilient Buildings and Construction Sector.

21. Zozuláková, Silvia &Bagoňa, Miloslav. (2019). Gas filling in glass system. International Review of Applied Sciences and Engineering, 10, 1-8.
22. Cho, K.; Cho, D.; Koo, B.; Yun, Y (2023). Thermal Performance Analysis of Windows, Based on Argon Gas Percentages between Window Glasses. Buildings, 13, 2935.
23. Nettles, A. T. (1994). Basic Mechanics of Laminated Composite Plates. NASA Marshall Space Flight Center, Alabama 35812.
24. STN EN 1991-1-4(730035)Eurocode 1: Actions on structures. Part 1-4: General actions. Wind actions.
25. STN 73 0540-2+Z1+Z2: Thermal performance of buildings and components.

JÁN KANÓCZ*, VIKTOR KARĽA
TECHNICAL UNIVERSITY OF KOŠICE
FACULTY OF ART
WATSONOVA 4, SK-042 00 KOŠICE
SLOVAK REPUBLIC
Corresponding author: jan.kanocz@tuke.sk

MICHAL TOMKO, TOMÁŠ BAROŠ, VIKTÓRIA BAJZECEROVÁ
TECHNICAL UNIVERSITY OF KOŠICE
FACULTY OF CIVIL ENGINEERING
VYSOKOŠKOLSKÁ 4, SK-042 00 KOŠICE
SLOVAK REPUBLIC